Vorticity Control

DORON NOF

Department of Oceanography, The Florida State University, Tallahassee, FL 32306

(Manuscript received 30 October 1986, in final form 18 May 1987)

ABSTRACT

A nonlinear one-layer model is considered in order to describe the way that water with a relative vorticity intrudes into an otherwise stagnant channel. The channel has a uniform depth (D) and width (L) and the fluid is taken to be inviscid. The intruding fluid is separated from the (initially stagnant) water in the channel by a free dividing streamline that corresponds to a "vorticity front." This front intersects the channel wall (at the head of the intrusion) and extends backwards upstream. As the fluid with relative vorticity is intruding into the channel, the fluid with no relative vorticity (i.e., the fluid present in the channel prior to the intrusion) escapes in the opposite direction. This flow compensates for the fluid displaced by the advancing intrusion. Solutions for steadily propagating intrusions are obtained analytically by equating the flow-force ahead of and behind the intrusion. Namely, steady state solutions correspond to a balance between the forward momentum flux and the form drag exerted on the intrusion by the escaping fluid. The nature of the intersection of the front with the wall is analyzed by methods similar to those employed by Stokes for analyzing the maximum steepness of surface gravity waves.

It is found that the vorticity in the intruding fluid "controls" the amount of fluid that flows through the channel. When the vorticity (ζ) of the intruding fluid is uniform, the width of the intrusion is always 2/3 of the channel width and the net volume flux of the intruding fluid is $(2/27)\zeta DL^2$. In the presence of weak dissipation, the channel can can transfer an amount less than $(2/27)\zeta DL^2$, but, under no circumstances can the channel transfer an amount larger than that. The maximum volume flux is much smaller than the flux associated with the so-called hydraulic control $\{\sim O[(gD)^{1/2}DL]\}$, which corresponds to the flux of an intrusion without any relative vorticity. When $\zeta \sim O(f)$, the ratio between the maximum flux allowed by the vorticity control to the flux allowed by the hydraulic control is equivalent to about 1/10 of the ratio between the channel width and the barotropic deformation radius. Hence, for midlatitude channels, the vorticity control may limit the flux *to a few percent* of that associated with the hydraulic control.

Possible application of this theory to various oceanic situations is mentioned.

1. Introduction

a. General description

When fluid with relative vorticity intrudes into a barotropic channel, it is pressed by the ambient fluid against one of the channel walls. Because of the excess pressure behind, it propagates along the wall and forms a "nose" at the leading edge. As the nose advances, the ambient fluid escapes to compensate for the intruding mass. The speed at which the leading edge advances, and the associated mass flux through the channel is the focus of our study.

b. Background

The way that geographical constrictions affect the flow in the ocean has been studied by many investigators. Much attention has been devoted to the so-called "hydraulic control" and its application to sea straits (e.g., Stern 1972, Whitehead et al. 1974, Gill 1977, Sambuco and Whitehead 1976, Stern 1974, Armi 1986, Armi and Farmer 1986, Farmer and Armi 1986, Pratt 1986, 1984, 1983, Borenas and Landberg 1986). The basic idea behind these studies is that the maximum flux through many straits is "controlled" in a similar way to the flow through a weir in a nonrotating flow.[1] The latter is associated with a Froude number (U^2/gD, where U is the speed, g the gravitational acceleration, and D is the depth) of unity, i.e., there is a stationary gravity wave at the constriction. In view of this, the mass transport associated with a hydraulically controlled flow is $(gD)^{1/2}DL$, where L is the width of the constriction.

Recently, another kind of "control" has been found (Garrett and Toulany 1982, Garrett 1983, Garrett and Majaess 1984, Toulany and Garrett 1984). It is called "geostrophic control" and, as in the hydraulic control case, is associated with the flow through a channel connecting two neighboring basins. The essence of this control is that the sea-level difference across a strait *cannot be larger* than the sea-level difference between the connected basins. The channel mass flux associated

[1] For many years, the nonrotating problem has been the subject of investigation by hydraulic engineers and, consequently, it received the name "hydraulic control." Traditionally, the application of this idea to large scale rotating flows in the ocean has also been called "hydraulic control" even though the word hydraulic is usually associated with smaller-scale manmade structures.

with a barotropic flow that is geostrophically controlled is,

$$Q = g\tilde{\eta}D/f, \quad (1.1)$$

where $\tilde{\eta}$ is the sea-level difference between the connecting basins, and f is the Coriolis parameter. The flow through broad and short gaps that do not resemble a channel is also geostrophically controlled in the sense that the flux is solely determined by the sea-level difference between the two basins (Nof and Olson 1983, Nof and Im 1985).

c. *Present approach*

In this paper we shall show that barotropic intrusions through channels are subject to another kind of control. This third type of control is related to the way that the vorticity controls the speed and flux. We shall see that, while the excess pressure behind the intrusion causes the flow, it does not control its speed and flux. In contrast to the hydraulic control and the geostrophic control (both of which are associated with the gravitational acceleration), the barotropic intrusion of fluid with relative vorticity is entirely dominated by the vorticity.

To show this, the following methods will be used. First, the nature of the intersection of the front with the channel wall is examined. Using methods similar to those employed by Stokes (1847) for studying the maximum steepness of gravity waves, it is shown that such an intersection is also a stagnation point and that the intersection angle is 90°. The intrusion propagation speed is then computed by equating the integrated flow-force (ahead of and behind the intrusion) and conserving the energy of the flow. This computation shows that the propagation speed is related to the vorticity of the intrusion and that the intrusion must occupy two-thirds of the channel width. Finally, allowance is made for weak dissipation and it is shown that, a) the propagation speed is slower than the speed associated with energy conservation, and b) the width is smaller than two-thirds of the channel width. It is shown that, under no circumstances, is the speed faster than the one associated with conservation of energy. Similarly, the width can never be greater than two-thirds of the channel width.

Our analysis is organized as follows. The formulation of the problem is presented in section 2 and the behavior of the intersecting front is analyzed in section 3. Section 4 includes the solution for an energy conserving flow and section 5 addresses the possible modifications due to the presence of dissipation. Section 6 includes the discussion; the results are summarized in section 7.

2. Formulation

Consider the one-layer system shown in Figs. 1 and 2. Our model is frictionless and hydrostatic but the motions are not constrained to be quasi-geostrophic in the sense that the Rossby number is not necessarily small. Initially, a gate separates the fluid in the inner basin from that in the outer basin and both fluids are at rest. The level of the free surface in the inner basin is higher than that of the outer basin (by $\tilde{\eta}$) and the (flat) inner basin bottom is shallower (i.e., $\Delta H > 0$) than that of the channel. We shall see later that it is also possible to consider cases where $\Delta H < 0$ but this requires the gate to be situated near the *left* bank.

At $t = 0$ the gate is lifted and, subsequently, fluid from the inner basin starts penetrating into the infinitely long channel (the outer basin). It is expected that, simultaneously, gravity waves will be generated. Within a short period, some of these waves will be modified into Kelvin waves that will propagate along the channel. Because of the depth difference between the basins, the intruding fluid has vorticity whereas the ambient fluid does not. Consequently, there is a "vorticity front," i.e., a free dividing streamline which separates the inner fluid (with relative vorticity) from the outer fluid (without relative vorticity). The structure of the front will become apparent shortly; for other flows with vorticity fronts the reader is referred to Stern and Pratt (1985) and Stern and Voropayev (1984).

After a period of $O(f^{-1})$, the intrusion head will reach a steady propagation rate and it is this state that we shall focus on (Fig. 3). Far from the intrusion head [i.e., several channel width (L) away] the steady upstream and downstream flows are expected to be in geostrophic balance because, in these regions, the geometry tends to force the flow to be one-dimensional. We shall view the intrusion process from a coordinate system traveling with the intrusion nose at the speed C. The x and y axes are directed along and across the channel, and the system rotates uniformly at $f/2$ about the z axis. In our moving coordinate system the motion of both the inner and outer fluid appears to be steady and the equations of motion are the usual shallow water equations,

$$u\frac{\partial u}{\partial x} + v\frac{\partial u}{\partial y} - fv = -g\frac{\partial \eta}{\partial x}$$

$$u\frac{\partial v}{\partial x} + v\frac{\partial v}{\partial y} + f(u + C) = -g\frac{\partial \eta}{\partial y}$$

$$\frac{\partial}{\partial x}(hu) + \frac{\partial}{\partial y}(hv) = 0,$$

where h is the total fluid depth, u and v are the horizontal two-dimensional velocity components [$u = u(x, y)$; $v = v(x, y)$], η the free surface displacement ($\eta \ll H$, $\eta = 0$; $x \to \infty$), and C is the intrusion propagation rate. These equations can be manipulated to give the steady potential vorticity equations and the Bernoulli integral,

$$\nabla \cdot \left(\frac{\nabla \tilde{\psi}}{h}\right) + f = hk(\tilde{\psi}) \quad (2.1a)$$

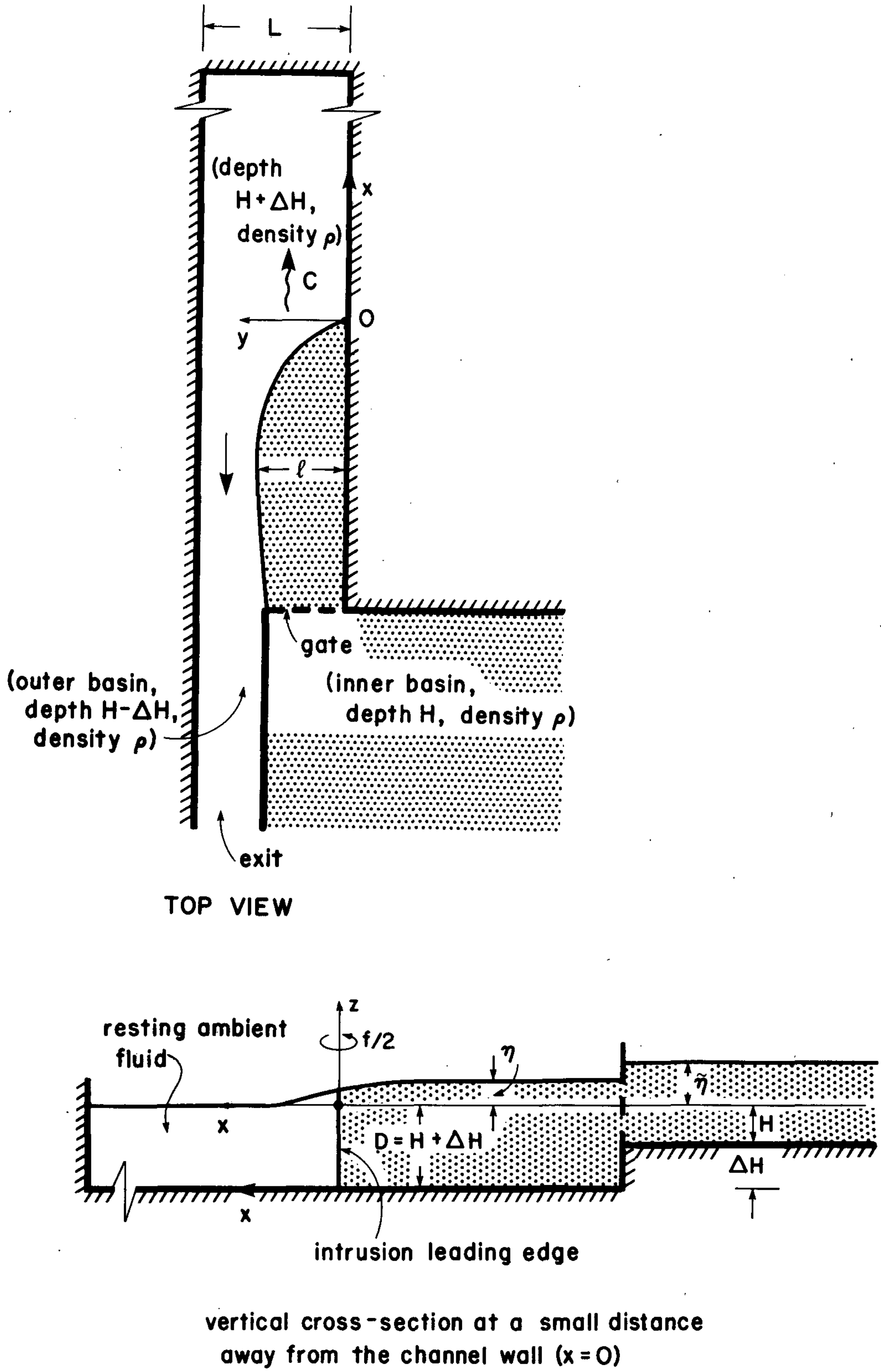

FIG. 1. Schematic diagram of the barotropic flow under study. At $t < 0$ there is no motion and the pressure associated with the sea-level difference between the two basins ($\tilde{\eta}$) is exerted on the gate. At $t = 0$ the gate is removed and the anomalous water (shaded) intrudes into the infinitely long channel that is blocked at the end. After some time a steady propagation rate will be reached. "Wavy" arrows denote propagation and solid arrows correspond to particles speed. Surface displacements shown in the vertical cross section are exaggerated; in reality $\eta \ll H$; ΔH.

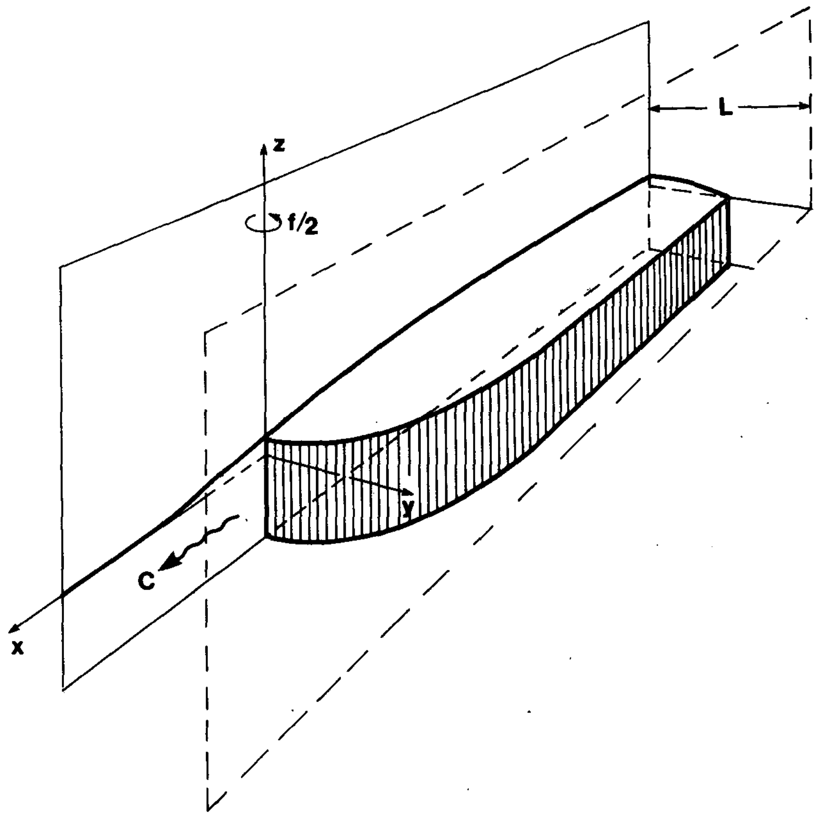

FIG. 2. A three-dimensional view of the intrusion leading edge.

$$\frac{1}{2}\left[\left(\frac{1}{h}\frac{\partial\tilde{\psi}}{\partial x}\right)^2+\left(\frac{1}{h}\frac{\partial\tilde{\psi}}{\partial y}\right)^2\right]+g\eta+fCy=B(\tilde{\psi}), \quad (2.1\text{b})$$

where the streamfunction $\tilde{\psi}$ is defined by

$$\frac{\partial\tilde{\psi}}{\partial y}=-uh; \quad \frac{\partial\tilde{\psi}}{\partial x}=vh,$$

and $K(\tilde{\psi}) = dB(\tilde{\psi})/d\tilde{\psi}$. Note that the potential vorticity equation is not affected by the migration whereas the Bernoulli integral *is altered* by the drift; as a result of the migration the Bernoulli integral has an additional term fCy.

a. Governing equations

With the rigid lid approximation ($\eta \ll \Delta H$), the transient potential vorticity equation $D[(v_x - u_y + f)/h]/Dt = 0$ gives for the outer fluid,

$$\nabla^2\psi_o=0, \quad (2.1\text{c})$$

where $\partial\psi_o/\partial y = -u$, $\partial\psi_o/\partial x = v$. The subscript "$o$" denotes that the variable in question is associated with the "outer" fluid; the subscript "i" will be used later to indicate association with the "inner" fluid. In deriving (2.1), it has been taken into account that the outer fluid was initially at rest so that the initial (and final) potential vorticity is $f/D = f/(H + \Delta H)$. Similarly, for the inner fluid, the potential vorticity equation gives,

$$\nabla^2\psi_i=f\Delta H/H. \quad (2.2)$$

b. Boundary conditions

The boundary conditions are that the walls ($y = 0$, $y = L$) are streamlines and that far upstream,

$$u_o=-C; \quad x\to\infty; \quad 0\leqslant y\leqslant L. \quad (2.3)$$

Downstream in the outer fluid [cross section (d), Fig. 3] we have (by the continuity equation),

$$u_o=-C\left(\frac{L}{L-l}\right); \quad x\to-\infty; \quad l\leqslant y\leqslant L. \quad (2.4)$$

For the downstream inner fluid ($x \to -\infty$) we have [by (2.2) and integration of the continuity equation from $y = 0$ to $y = l$],

$$u_i=-f\frac{\Delta H}{H}(y-l/2); \quad x\to-\infty; \quad 0\leqslant y\leqslant l. \quad (2.5\text{a})$$

Recall now that the solution of (2.1c) and (2.2) requires knowledge of the streamfunction (or its derivative) along all the boundaries. Our previous consid-

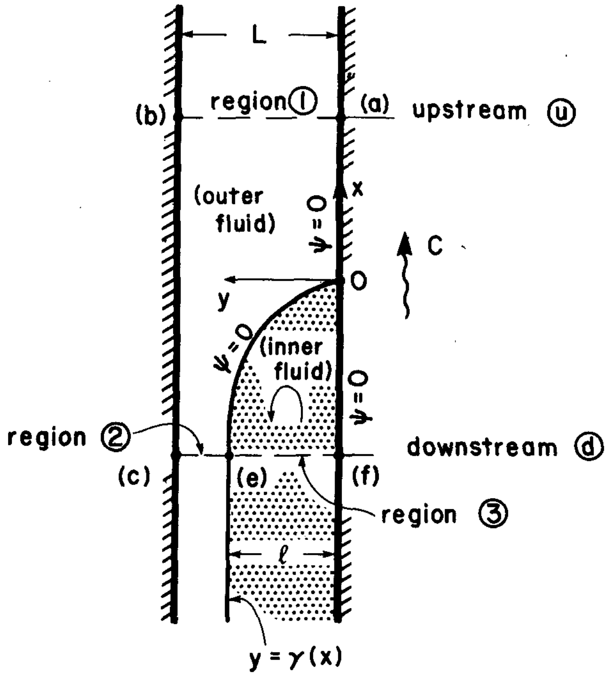

FIG. 3. The cross section ahead (upstream) and behind (downstream) the intrusion. Note that the terms "upstream" and "downstream" are used here with reference to the ambient fluid rather than the intrusion. Cross sections ⓤ and ⓓ are located several channel widths away from the head and leading edge. They include region ① [connecting points (a) and (b)], region ② [connecting points (c) and (e)] and region ③ [connecting points (e) and (f)]. The streamfunction ψ is defined to be zero along the right bank (looking at the direction of propagation). As before, wavy arrows denote propagation and solid arrows correspond to particles speed.

erations and (2.3–2.5) indicate that, as required, we know the distribution of ψ along all the boundaries,

outer fluid:

$$\psi_o=0; \quad y=0, \quad \infty>x\geqslant 0 \tag{2.6a}$$

$$\psi_o=Cy; \quad 0\leqslant y\leqslant L, \quad x\to\infty \tag{2.6b}$$

$$\psi_o=CL; \quad y=L, \quad \infty>x>-\infty \tag{2.6c}$$

$$\psi_o=C\left(\frac{L}{L-l}\right)(y-l); \quad l\leqslant y\leqslant L, \quad x\to-\infty \tag{2.6d}$$

$$\psi_o=0; \quad y=\gamma(x), \quad 0\geqslant x>-\infty \tag{2.6e}$$

inner fluid:

$$\psi_i=0; \quad y=0, \quad 0\geqslant x\to-\infty \tag{2.7a}$$

$$\psi_i=0; \quad y=\gamma(x), \quad 0\geqslant x\to-\infty \tag{2.7b}$$

$$\psi_i=\frac{f\Delta H}{H}\frac{y}{2}(y-l); \quad \gamma(-\infty)\geqslant y\geqslant 0, \quad x\to-\infty. \tag{2.7c}$$

However, although the distribution of ψ is known, the location of the streamline $y=\gamma(x)$ is not known a priori. Since the position of the free separating streamline $y=\gamma(x)$ is not known in advance but rather must be solved as part of the problem, we need an additional boundary condition on ψ. This is supplied by the condition that the sea level (i.e., the pressure) must be continuous across the front $y=\gamma(x)$,

$$\eta_i=\eta_o; \quad y=\gamma(x); \quad -\infty<x\leqslant 0. \tag{2.8}$$

Relation (2.8) can be expressed in terms of ψ by using a modification of the Bernoulli integral (2.1b),

$$\frac{1}{2}(u^2+v^2)+g\eta+fCy=B(\psi), \tag{2.9}$$

where $\psi=\tilde{\psi}/(H+\Delta H)$ and $D=(H+\Delta H)\approx h$.

In general, $B(\psi)$ is to be determined from the upstream conditions. As we shall see shortly, the upstream conditions for the outer fluid allow a detailed computation of B but this is not the case for the inner fluid. For the outer fluid, the upstream conditions ($u_o=-C$; $\psi_o=Cy$) give,

$$C^2/2+f\psi_o=B_o(\psi_o)$$

so that

$$B_o(0)=C^2/2. \tag{2.10}$$

For the inner fluid, however, it is not possible to a priori determine the value of $B_i(\psi)$ because the sea level at $x\to-\infty$ is not known. Namely, we have

$$B_i(0)=g\eta_{if}+\frac{f^2l^2}{8}\left(\frac{\Delta H}{H}\right)^2, \tag{2.11}$$

where η_{if} [the sea level at (f), Fig. 3] is a constant to be determined *as a part of the solution.*

Relations (2.11), (2.10) and (2.9) allow us to express the boundary condition (2.8) in the form,

$$\frac{1}{2}\left[\left(\frac{\partial\psi_o}{\partial x}\right)^2+\left(\frac{\partial\psi_o}{\partial y}\right)^2\right]-C^2/2=\frac{1}{2}\left[\left(\frac{\partial\psi_i}{\partial x}\right)^2+\left(\frac{\partial\psi_i}{\partial y}\right)^2\right]-\left[g\eta_{if}+\frac{fl^2}{8}\left(\frac{\Delta H}{H}\right)^2\right]; \quad y=\gamma(x), \tag{2.12}$$

which is the desired additional condition on ψ.

This condition is highly *nonlinear*; it represents the main difficulty associated with the solution of the linear governing equations (2.1) and (2.2). It is important to realize that in the usual quasi-geostrophic theory the terms associated with the square of the velocity are *neglected.* This is so because for quasi-geostrophic flows the ratio of u^2 (or v^2) to the other terms in the Bernoulli integral (e.g., fCy) is of the order of the Rossby number which is taken to be small. In our case, however, the Rossby number is not small because the square of the velocity [$O(fL)^2$] is of the *same* order as fCL [since $C\sim O(fL)$].

Solutions involving such free separating streamlines are notorious because, as already mentioned, the position and slope of the streamline are not known in advance and the nonlinear terms cannot be neglected (e.g., see Benjamin 1968, Batchelor 1967). There is no direct way to compute the variables associated with the separating streamline and it is usually necessary to "guess" the value of the variables in question. To avoid the above difficulty, we shall seek solutions for the intrusion speed (C) and width (l) *without* solving for the whole field. We shall see that, by conserving the flow-force in cross sections ⓤ and ⓓ, and by analyzing the nature of the solution in the vicinity of point O (Fig. 3), it is possible to determine C and the position of the streamline at $x \rightarrow -\infty$ without finding the entire solution.

3. The intersection of the vorticity front [$y = \gamma(x)$] with the wall

In this section we shall show that the point at which the vorticity front intersects the wall is a double stagnation point, i.e., both the inner and the outer fluid stagnate there (Fig. 4). We shall also show that the intersection angle must be exactly 90°.

We begin by noting that the nature of the intersection is not a priori obvious. For example, it appears that at 0 the slope of the free dividing streamline could be either zero (Fig. 5b) or π (Fig. 5a). In the latter case only the intruding fluid would stagnate at 0 (because the outer fluid can slide along) whereas in the former case only the ambient fluid would stagnate there. To compute the intersection angle α we shall follow the technique used by Stokes (1847) to determine the angle associated with the maximum steepness of surface gravity waves. Stokes' method involves an analysis which combines application of conformal mapping and the Bernoulli integral. Using these procedures he determined that the angle of sharp crested waves must be $2\pi/3$. Von Kármán (1940) later used the same method to determine the intersection angle of the front associated with the head of a gravity current; he found that this angle must be $\pi/3$.

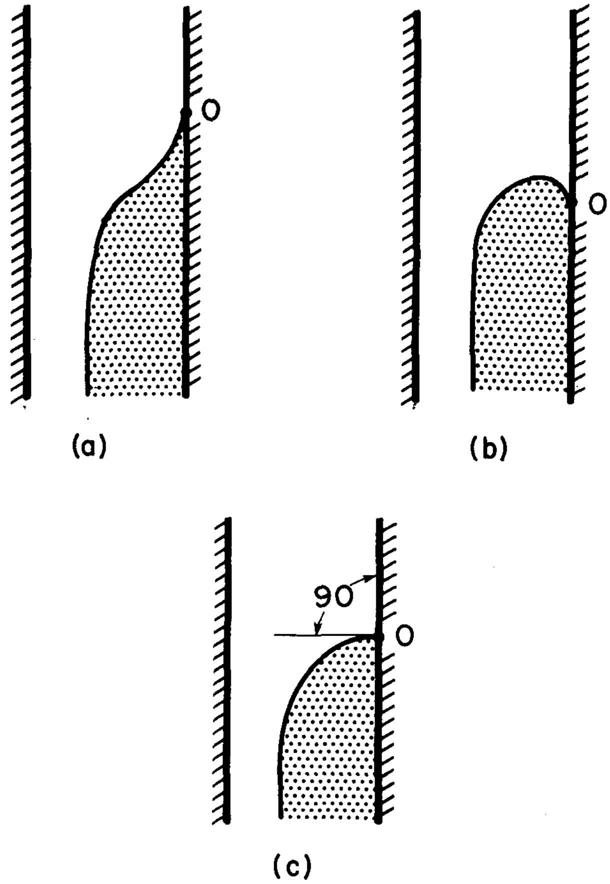

FIG. 5. A sketch of three intersections of the vorticity front $y = \gamma(x)$ with the wall. In (a) $\alpha = \pi$, the ambient fluid (not shaded) does not stagnate at 0 but the anomalous fluid (shaded) does come to rest there. This results from the fact that only the anomalous fluid has a discontinuity in the adjacent streamline slope. In (b) $\alpha = 0$, the opposite situation exists, i.e., the anomalous fluid does not stagnate whereas the ambient fluid does. As shown in the text, none of these situations is physically possible. Instead, the intersection angle is $\pi/2$ so that there is a discontinuous slope for both fields and both fluids stagnate at 0 [situation (c)].

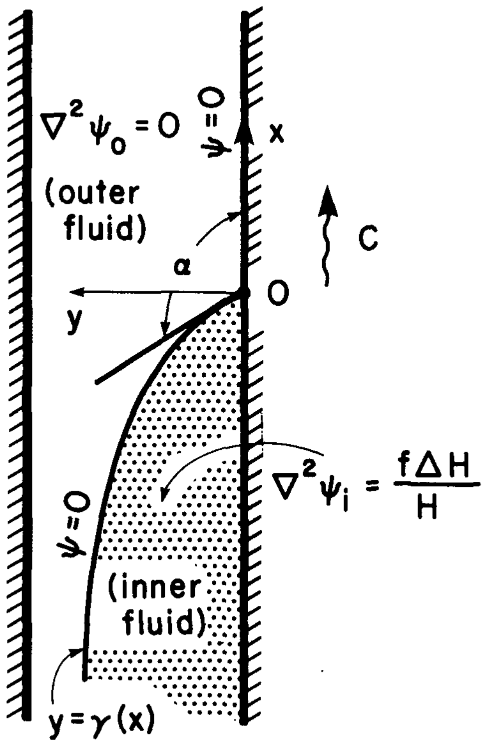

FIG. 4. Schematic diagram of the intersection between the free dividing streamline [$y = \gamma(x)$] and the wall ($y = 0$). Note that it is not a priori obvious that 0 is a stagnation point for both fluids because the situations displayed in Fig. 5a ($\alpha = \pi$) or Fig. 5b ($\alpha = 0$) appear also to be possible. Our analysis shows, however, that $\alpha = \pi/2$ (Fig. 5c) so that both fluids must stagnate at 0.

a. The outer flow near point 0

In the immediate vicinity of 0, the flow of both fluids behaves like a flow inside a corner, i.e., the outer fluid flows inside a corner with an angle α whereas the inner fluid flows inside a corner of $(\pi - \alpha)$. The outer fluid is governed by $\nabla^2\psi_o = 0$ so that one can derive its solution with the aid of conformal mapping (e.g., see Batchelor 1970, p. 409). Specifically, for a flow inside a corner the complex potential w ($=\phi + i\psi_o$, where ϕ is the potential and ψ_o the streamfunction) is an analytic function of z ($=x + iy$) and we have,

$$w(z) = Az^n, \tag{3.1}$$

where A and n are real constants. If r, θ are polar coordinates in the z plane, we have $z = re^{i\theta}$ and

$$\psi_o = Ar^n \sin n\theta. \tag{3.1a}$$

This expression for ψ vanishes for all r when $\theta = 0$ and $\theta = \pi/n$. Hence, (3.1) and (3.1a) provide a representation of potential flow in the region between two straight zone flux boundaries intersecting at an angle π/n. The speed of the flow q_o is given by

$$q_o = \left|\frac{dw}{dz}\right| = |nA|r^{n-1}, \tag{3.1b}$$

so that along the separating streamline $\psi_o = 0$ ($y = x \times \tan\alpha$) the outer velocity is proportional to nAy^{n-1} and the velocity square $(u_o^2 + v_o^2)$ is proportional to $y^{2(n-1)}$.

b. The inner flow in the vicinity of 0

The inner fluid is governed by the Poisson equation $\nabla^2\psi_i = f\Delta H/H$ so that the solution is a sum of a particular solution (whose Laplacian gives $f\Delta H/H$) and a homogeneous solution (ψ_{ih}) similar to (3.1), i.e.,

$$w(z) = Bz^m; \quad \psi_{ih} = Br^m \sin m\theta, \tag{3.2}$$

where $m = n/(n - 1)$ since $\pi/m + \pi/n = \pi$.

As before, $(u_{ih}^2 + v_{ih}^2)$ is proportional to $y^{2(m-1)}$ along $y = x \tan\alpha$. The particular solution (ψ_{ip}) satisfying the boundary condition $\psi_{ip} = 0$ on $y = 0$ and $y = x \tan\alpha$ is

$$\psi_{ip} = \frac{f\Delta H}{2H} y(y - x \tan\alpha). \tag{3.3}$$

This shows that along $y = x \tan\alpha$, u_{ip} and v_{ip} are proportional to y. Since the inner homogeneous speed is proportional to $y^{(m-1)}$ and the inner particular speed is proportional to y, it follows that the square of the total inner speed $(u_i^2 + v_i^2)$ must be proportional to $y^{2(m-1)}$, y^2 and y^m.

c. Matching of the two flows

Leaving the above information aside for a moment we note that the Bernoulli integrals for the free separating streamline are

$$\frac{1}{2}(u_o^2 + v_o^2) + fCy + g\eta_o = B_o(0) \tag{3.4a}$$

$$\frac{1}{2}(u_i^2 - v_i^2) + fCy + g\eta_i = B_i(0), \tag{3.4b}$$

where (3.4a) corresponds to the inner fluid and (3.4b) to the outer. Since $\eta_i = \eta_o$ along $y = \gamma(x)$, (3.4) give,

$$(u_o^2 + v_o^2) - (u_i^2 + v_i^2) = 2[B_o(0) - B_i(0)]; \quad y = \gamma(x). \tag{3.5}$$

Recall now that along $y = x \tan\alpha$ the square of the outer speeds $(u_o^2 + v_o^2)$ is proportional to $y^{2(m-1)}$, y^2 and y^m. Since the right-hand side of (3.5) is a constant, and, hence, is free of y, the left-hand side must also be free of y implying that all terms involving powers of y must cancel each other. This can only happen if $(u_o^2 + v_o^2)$ and $(u_i^2 + v_i^2)$ have terms with *equal* powers of y. It is easy to show that when $m = n = 2$, the above condition is satisfied. Under such circumstances all terms in $(u_i^2 + v_i^2)$ and $(u_o^2 + v_o^2)$ are proportional to y^2. The condition $m = n = 2$ implies that the angles associated with the flows in both corners are $\pi/2$. We, therefore, conclude that,

$$\alpha = \pi/2. \tag{3.6}$$

Since α is not zero (Fig. 5b) or π (Fig. 5a), the intersection of the free separating streamline with the wall must represent a stagnation point for both fluids.

Strictly speaking, for $y \sim O(L)$, the offshore velocity component associated with the particular inner solution [i.e., $v_{ip} = \partial\psi_{ip}/\partial x = -f(\Delta H/2H)y \tan\alpha$] goes to infinity as $\alpha \to \pi/2$. This does not present any difficulty because the analysis is supposed to be valid only near the wall where $y \to 0$. It is a simple matter to show that if the angle α is not exactly $\pi/2$ but, say, $\frac{1}{2}\pi(1 + \epsilon)$ then the off-shore velocity vanishes for all $y < \epsilon^\beta$ where $\beta > 1$. In other words,

$$\lim_{\epsilon\to 0} \epsilon^\beta \tan\left[\frac{\pi}{2}(1 + \epsilon)\right] = 0; \quad \beta > 1$$

suggesting that, within a radius of $O(\epsilon^\beta)$ from the origin, our analysis is valid.

4. Solution

As mentioned in sections 2 and 3, finding the complete solution analytically is (probably) impossible due to the nonlinear boundary condition (2.12). It is, however, possible to determine analytically the most important aspects of the intrusion—its propagation speed C and its upstream width l. This can be done by, (i) conserving energy along the walls and the separating streamline, (ii) equating the flow-forces in cross sections ⓤ and ⓓ, and (iii) taking into account that 0 is a stagnation point.

a. Energy conservation

Application of the Bernoulli integral to the streamlines connecting (a–e), (b–c), and (e–f) (see Fig. 3) give,

$$\frac{C^2}{2}=\frac{C^2}{2}\left(\frac{L}{L-l}\right)^2+fCl+g\eta_{oe} \quad (4.1)$$

$$\frac{C^2}{2}=\frac{C^2}{2}\left(\frac{L}{L-l}\right)^2+g\eta_{oc} \quad (4.2)$$

$$u_{ie}^2/2+fCl+g\eta_{ie}=u_{if}^2/2+g\eta_{if}, \quad (4.3)$$

where, as before, the subscripts "o" and "i" correspond to the outer and inner fluids and the subscripts "e" and "f" correspond to points e and f (Fig. 3).

Recall that, in the moving frame of references, the solution for the upstream field of the inner fluid is antisymmetric with respect to $y = l/2$ [see (2.5a)] so that (4.3) reduces to,

$$fCl+g\eta_{ie}=g\eta_{if}. \quad (4.3a)$$

b. Momentum

To obtain the flow-forces ahead of and behind the intrusion, the x momentum equation for each fluid is integrated over the area, i.e.,

$$\left.\begin{aligned}\iint_{s_o}\left(u_o\frac{\partial u_o}{\partial x}+v_o\frac{\partial u_o}{\partial y}-fv_o+g\frac{\partial \eta_o}{\partial x}\right)dxdy=0\\ \iint_{s_i}\left(u_i\frac{\partial u_i}{\partial x}+v_i\frac{\partial u_i}{\partial y}-fv_i+g\frac{\partial \eta_i}{\partial x}\right)dxdy=0\end{aligned}\right\}, \quad (4.4)$$

where s_o and s_i are the areas confined by cross sections ⓤ and ⓓ (Fig. 3). By noting that $[\partial(u^2)/\partial x] + [\partial(uv)/\partial y] = (u\partial u/\partial x) + (v\partial u/\partial y)$ [in view of the continuity equation $(\partial u/\partial x + \partial v/\partial y = 0)$], using Stokes' theorem, and adding the two equations constituting (4.4), one finds,

$$\oint_{\phi_o}u_o^2dy-\oint_{\phi_o}u_ov_odx-f\oint_{\phi_o}\psi_ody+g\oint_{\phi_o}\eta_ody+\oint_{\phi_i}u_i^2dy-\oint_{\phi_i}u_iv_idx-f\oint_{\phi_i}\psi_idy+g\oint_{\phi_i}\eta_idy=0, \quad (4.5)$$

where ϕ_o and ϕ_i are the boundaries of the two regions. We now note that, $udy = udx$ along any streamline and that $\eta_i = \eta_o$ along the separating streamline [$y = \gamma(x)$]. These show that (4.5) can be reduced to,

$$\boxed{\int_0^L(u_o^2-f\psi_o+g\eta_o)dy=\int_l^L(u_o^2-f\psi_o+g\eta_o)dy+\int_0^l(u_i^2-f\psi_i+g\eta_i)dy. \quad (4.6)}$$

c. Stagnation at 0

Since both the outer and the inner speeds vanish at 0, it follows immediately from (3.4) and (2.10) that $B_i(0) = B_o(0) = C^2/2$. Also, (3.4) shows that,

$$u_o^2+v_o^2=u_i^2+v_i^2;\quad y=\gamma(x),\quad -\infty<x\leqslant 0$$

so that in the upstream region of the intrusion ($x \to -\infty$),

$$u_o^2=u_i^2;\quad x\to-\infty,\quad y=l. \quad (4.7)$$

Equation (4.7) has two roots,

$$u_o=u_i$$

$$u_o=-u_i. \quad (4.8)$$

Only the first root is physically realizable; the second involves a discontinuity in speed and is physically irrelevant because, it turns out that, it leads to absolute negative velocities near the right wall.

d. Derivation of solution

By incorporating (4.1)–(4.3) into (4.6), taking into account that $\eta = 0$ for all y at $x \to \infty$, and that the flows upstream and downstream are geostrophic (i.e., integration of the geostrophic relationship gives, $f\psi = g\eta + fCy +$ constant), one finds,

$$C=fl\frac{\Delta H}{2H\sqrt{3}}\left[\frac{L}{2l}+\left(\frac{L}{L-l}\right)^2\left(1-\frac{L}{2l}\right)\right]^{1/2}. \quad (4.9)$$

Relation (2.5a) and the physically relevant root of (4.7) give

$$C\left(\frac{L}{L-l}\right)=f\frac{\Delta H}{2H}l, \quad (4.10)$$

which upon substitution into (4.9), yields the equation,

$$\sqrt{3}\left(\frac{L}{l}-1\right)\left[\frac{L}{2l}+\left(\frac{L}{l}\right)^2\left(1-\frac{L}{2l}\right)\left(\frac{L}{l}-1\right)^2\right]^{1/2}-\frac{L}{l}=0. \quad (4.11)$$

The only nontrivial solution of (4.11) is

$$\boxed{L=3l/2}\quad, \quad (4.12)$$

and the associated migration speed C is,

$$\boxed{C=f\frac{\Delta H}{6H}l=f\frac{\Delta H}{9H}L}\quad. \quad (4.13)$$

The net transport of the inner (or outer) fluid is $\frac{2}{27}f(\Delta H/H)(H + \Delta H)L^2$ and, if we denote the relative vorticity of the inner fluid by $\zeta = f\Delta H/H$), then the flux can be expressed as,

$$\boxed{T=\frac{2}{27}\zeta(H+\Delta H)L^2}\quad. \quad (4.14)$$

The total transport of inner fluid into the channel is actually larger than that given by (4.14). It amounts to $\frac{8}{81}\zeta(H + \Delta H)L^2$; 25% of this transport [i.e., $\frac{2}{81}\zeta(H + \Delta H)L^2$] is detrained (as shown in Fig. 6) and the remaining proceeds into the channel.

Recall that the flow properties described by (4.12)–(4.14) are associated with *steady energy conserving flow*. Also, note that all the flow properties, as well as the transport, are independent of $\tilde{\eta}$, the sea-level difference between the basins. A question that comes immediately to mind is whether or not the actual transport can be different from that given by (4.14). For instance, what would happen if we throttle the escaping fluid? Or, equivalently, is it possible to force into the channel more fluid than that given by (4.14)? The answers to these questions are given in the next section; we shall see that weak dissipation allows for a smaller mass transport. However, under no circumstances is a larger transport possible.

5. The influence of weak dissipation

To examine the detailed role of weak dissipation and friction, it is necessary to include viscosity in the equations of motion and solve the problem accordingly. This general problem is rather complicated and is beyond the scope of this study. We shall, however, qualitatively examine the role of weak dissipation resulting from laterally breaking waves. The fact that lateral waves (i.e., lateral displacements of the vorticity front) can break is not new (see Stern 1985). It is, therefore, of interest to examine the changes that may consequently occur. Specifically, it is expected that, as a result of such an energy loss (see Fig. 7), the width of the intrusion will be different from that that was found earlier ($2L/3$), and the speed will be different from that given by (4.19). While it is clear that some changes will take place, the real question is whether or not C can *exceed* the speed given by (4.13) and whether l can be *greater* than $2L/3$. Our approach to the energy loss problem is very similar to that of Benjamin (1968) who computed the losses associated with the head of a gravity current. Although an attempt has been made to make the present paper self-contained, the reader may wish to consult Benjamin's work before proceeding to the subsequent discussion.

Suppose that the wave breaking occurs over a small region (as shown in Fig. 7) and that, as both fluids pass through the breaking-wave zone, they suffer a uniform energy loss δ. Under such conditions, the Bernoulli integrals (4.1)–(4.3) are modified to

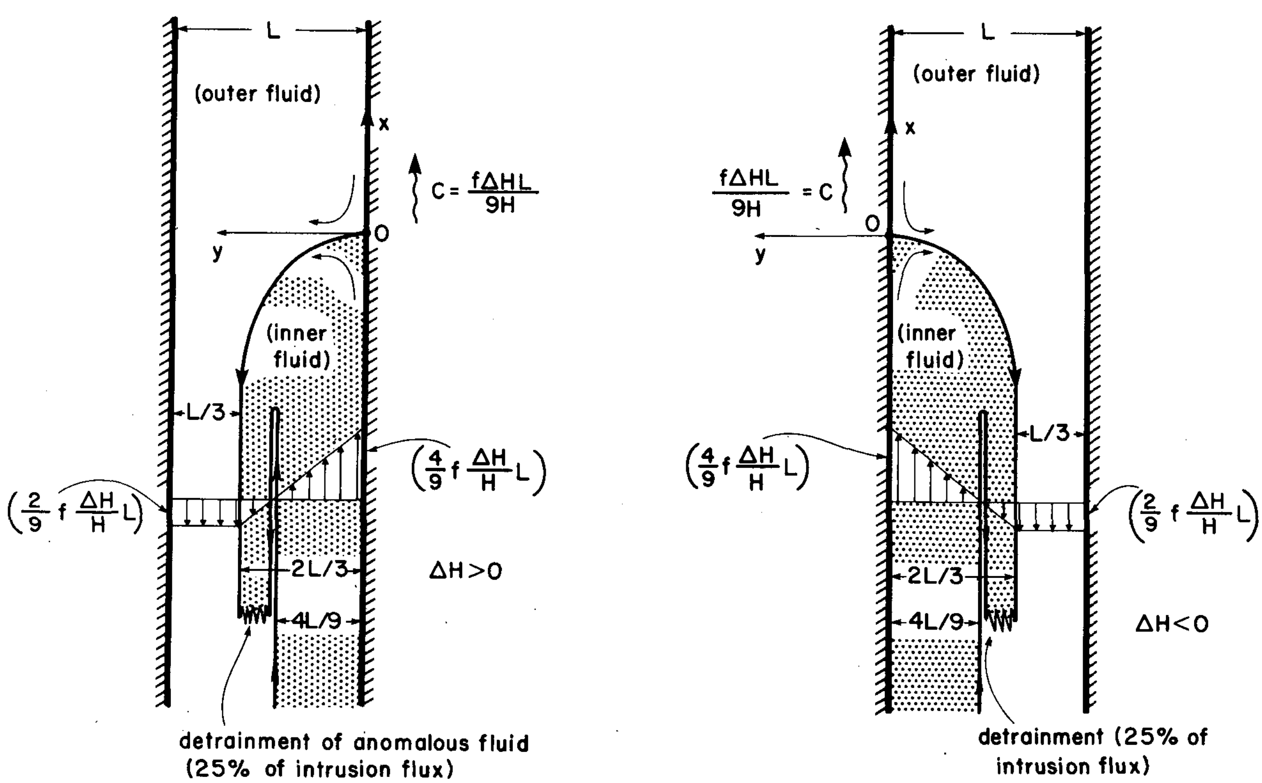

FIG. 6. The detailed structure of the intrusion. When $\Delta H > 0$, the anomalous vorticity is cyclonic and the intrusion propagates along the right wall (left panel) whereas when $\Delta H < 0$ (anticyclonic vorticity) the intrusion propagates along the left wall (right panel). Note that the speeds are those that are viewed from a *stationary* coordinate system.

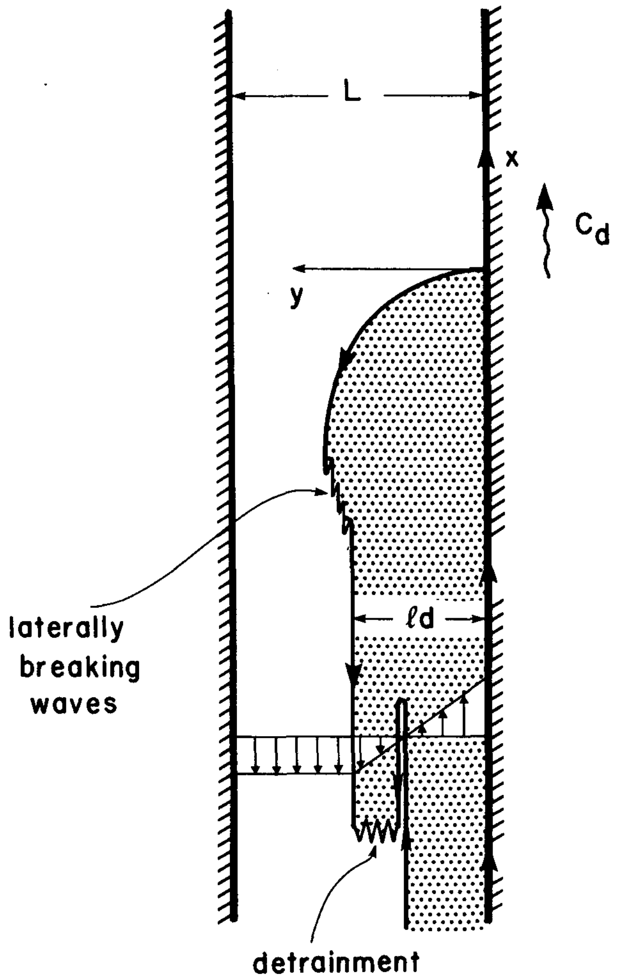

FIG. 7. A sketch of an intrusion with dissipation due to laterally breaking waves. The modified propagation speed is C_d and the modified width is l_d. As shown in the text, both quantities are smaller than their inviscid counterparts.

$$\frac{C_d^2}{2}-\delta=\frac{C_d^2}{2}\left(\frac{L}{L-l_d}\right)^2+fC_dl_d+g\eta_{oe} \tag{5.1}$$

$$\frac{C_d^2}{2}-\delta=\frac{C_d^2}{2}\left(\frac{L}{L-l_d}\right)^2+g\eta_{oe} \tag{5.2}$$

$$\frac{u_{ie}^2}{2}+fC_dl_d+g\eta_{ie}=\frac{u_{if}^2}{2}+g\eta_{if}, \tag{5.3}$$

where the subscript "d" indicates that the variable in question is associated with dissipation.

Suppose further that the role of dissipation is relatively small (i.e., $\delta \ll Cd^2/2$) so that the potential vorticity is not altered and the general structure of the solution in regions 1, 2 and 3 (Fig. 3) remains unchanged. This assumption is consistent with Nof's (1986) analysis which showed that potential vorticity can only be altered by high amplitude shock waves. Namely, it is expected that, in our problem, changes in potential vorticity would occur only if the lateral waves are large. With or without dissipation, the flow-force must, of course, be conserved and the nature of the stagnation point must also remain unaltered. By using this information and following a procedure identical to that presented in section 4, one ultimately finds

$$C_d=\left[f^2\left(\frac{\Delta H}{H}\right)^2 l_d^2/12-\delta\left(\frac{L-l_d}{l_d}\right)\right]^{1/2}\Bigg/ \left[\left(\frac{L}{L-l_d}\right)^2-\left(\frac{L}{L-l_d}\right)^2\frac{L}{2l_d}+\frac{L}{2l_d}\right]^{1/2}, \tag{5.4}$$

and, as before,

$$C_d\left(\frac{L}{L-l_d}\right)=f\frac{\Delta H}{2H}l_d. \tag{5.5}$$

Equations (5.4) and (5.5) constitute the solution for C_d and l_d. For simplicity, one may express C_d and l_d as

$$C_d=C+C'; \quad l_d=l+l', \tag{5.6}$$

where C' and l' are small perturbations. Upon substitution of (5.6) into (5.4) and (5.5) one finds

$$C'=-\sqrt{3}\delta\left(\frac{L}{L-l^{-1}}\right)\Bigg/\left[\left(\frac{L}{L-l}\right)^2-\left(\frac{L}{L-l}\right)^2 \frac{L}{2l}+\frac{L}{2l}\right]^{1/2} f\frac{\Delta H}{H}l=\frac{-3\delta}{4f(\Delta H/H)L} \tag{5.7a}$$

$$l'=\frac{-4\delta L}{f^2(\Delta H/H)^2} \tag{5.7b}$$

so that

$$\left.\begin{aligned} C_d&=\frac{f(\Delta H/H)L}{9}-\frac{3\delta}{4f(\Delta H/H)L}\\ l_d&=\frac{2}{3}L-\frac{4\delta L}{f^2(\Delta H/H)^2}\end{aligned}\right\}. \tag{5.8}$$

We see that both C_d and l_d are *smaller* than those associated with the nondissipative state. We, therefore, conclude that the actual net transport can be *smaller* than $\frac{2}{27}\zeta DL^2$ but, under no circumstances, can it be greater. Evidently, if the total flux from the inner basin to the channel is restricted to less than the inviscid amount ($\frac{8}{81}\zeta DL^2$) then there will be laterally breaking waves and a new steady propagation rate will be reached. However, attempts to force into the channel amounts *larger* than ($\frac{8}{81}\zeta DL^2$) (by, say, increasing the upstream sea level) will be fruitless because alteration of the upstream conditions will take place.

6. Discussion

a. General comments

In the foregoing sections it has been demonstrated that an intrusion with cyclonic vorticity ($\Delta H > 0$) must propagate along the *right* channel wall. It is a simple matter to show that, similarly, when the vorticity is anticyclonic ($\Delta H < 0$) the intrusion can only propagate along the *left* wall (Fig. 6). Under the latter conditions our inner basin must, of course, also be located on the left-hand side. In both cases, 25% of the fluid is detrained, i.e., it is released from the inner fluid and absorbed by the outer fluid. A similar detrainment has been found in baroclinic intrusions (e.g., see Stern et al. 1982) so that its presence here is not surprising.

It is important to realize that the entire dynamics of the problem is "controlled" by the vorticity of the intruding fluid. The intrusion occupies two-thirds of the channel width and propagates at $(f\Delta H/9H)L$; the corresponding *net* transport is $2f\Delta HDL^2/27H$. For a midlatitude channel 10 km wide and 200 m deep, and a step (ΔH) of 50 m, the propagation rate is relatively slow, about 3 cm s^{-1}. Had the intrusion been controlled by gravity, rather than vorticity, then the propagation rate would have been of the order of $(gH)^{1/2} - 30$ m s^{-1}.

In the absence of rotation, there is no free separating streamline and the flow is *uniform* downstream (Fig. 8). Consequently, there is no vorticity control; the only control that can be active is the hydraulic control. This implies that the maximum transport that can be forced through the channel is $(gD)^{1/2}DL/2$ corresponding to a stationary gravity wave at the exit [i.e., $u \sim (gD)^{1/2}$]. On the other hand, once rotation is introduced to the system ($f \neq 0$), the hydraulic control is no longer possible because the vorticity control is much more restrictive.

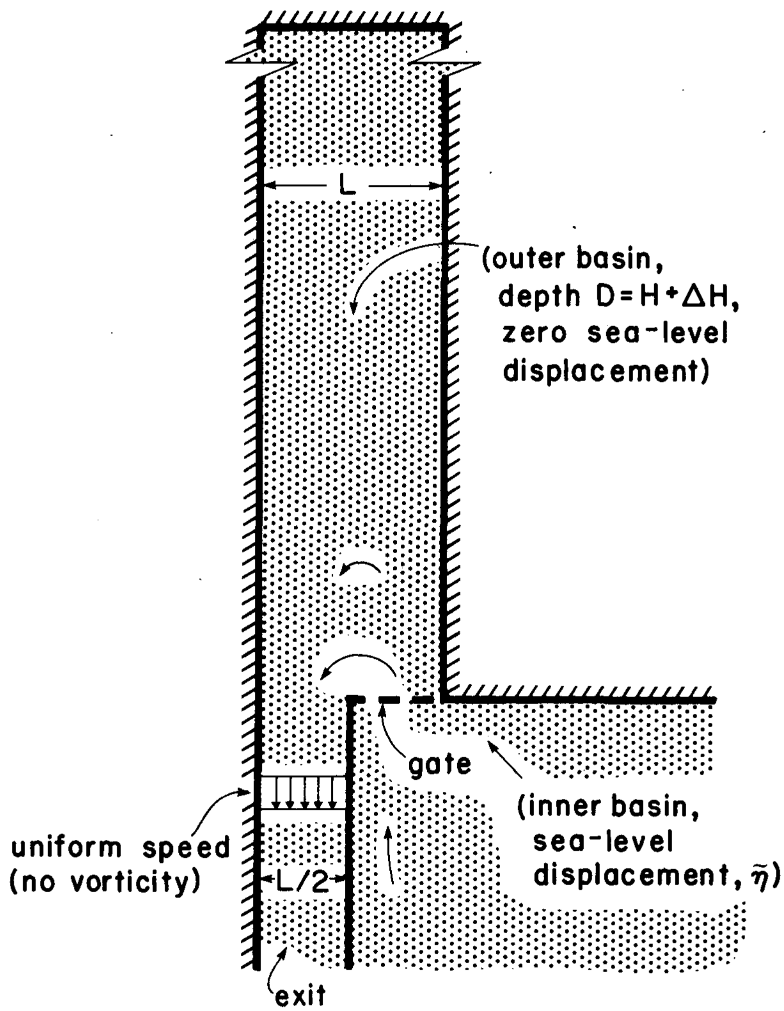

FIG. 8. Sketch of the nonrotating flow through the channel. According to the hydraulic control concept, the maximum flux that can be forced through the channel is $(gD)^{1/2}DL/2$ corresponding to $U = (gD)^{1/2}$ at the exit. Recall that the channel depth D equals $H + \Delta H$.

When the channel is of *finite* length, rather than infinitely long as we have assumed, the vorticity control will be temporary. It will only last until the intrusion reaches the end of the channel because once the intrusion head arrives at the end, there is no longer a simple intersection of the free separating streamline with the wall. After the nose reaches the exit, the hydraulic control or geostrophic control will start dominating the flow. If the sea-level difference between the basins ($\tilde{\eta}$) is relatively small so that the hydraulic control [$u \sim O(gD)^{1/2}$, $T = (gD)^{1/2}DL$] cannot be reached, the geostrophic control will dominate [$T = g\tilde{\eta}D/f$]. If, on the other hand, the sea-level difference between the basins is large and the channel width is $\sim O(gD)^{1/2}/f$, then the geostrophic control will not be active and the hydraulic control will take over. A detailed comparison of the three types of control is given in Table 1.

It is important to note that the lack of any transport for $\zeta \rightarrow 0$ in (4.14) is a direct consequence of the rigid-lid approximation. This approximation ($\eta \ll \Delta H$, H) essentially filters out gravity waves so that the classic hydraulic control (which is identified as the condition under which the advection equals the gravity wave speed) is also filtered out. In other words, our solution is only valid for large ΔH and cannot be used when $\Delta H < \eta$; under such conditions the free surface level cannot be neglected and must be taken into account.

b. Applications

It is expected that various oceanic channels may actually be affected by the newly proposed vorticity control. The flow in many channels and straits is barotropic [e.g., the tidal flow in the Johnstone Strait (Thompson 1976)] and variations in atmospheric pressure or tides are likely to cause transient intrusions into them. Unfortunately, there are no published reports on such barotropic intrusions. Since barotropic intrusions do not have any temperature signature (unless it is somehow compensated by salinity), they cannot be easily identified from satellite photographs. It is probably for this reason that barotropic intrusions have not been reported in the literature. Note, however, that it is not at all obvious whether a sufficient amount of baroclinicity can completely invalidate the vorticity control theory. Hopefully, this question will be answered in the future by further theoretical studies as well as field experiments.

It should also be pointed out that our particular geometrical configuration (Fig. 1) was chosen because of its conceptual simplicity. Strictly speaking, this geometry may be best realized in a laboratory setting rather than a geophysical application. It is believed, however, that the vorticity control theory will be valid even for different configurations provided that the outer fluid is somehow allowed to escape.

Our present study suggests that barotropic intrusions may be so slow (due to their relative vorticity) that they may actually choke the flow in channels and straits. That is to say, the vorticity control may allow only small and weak mass fluxes to pass through channels and straits even if the sea-level difference is relatively large. For instance, it is known that there is almost no flow through the Torres Strait (situated between Australia and New Guinea) even though there is a large sea-level difference between the two connected basins

TABLE 1. A comparison between the two known types of control (i.e., hydraulic and geostrophic) and the newly proposed vorticity control.

Type of control	Cause of control	Duration of control	Maximum transport	Reference
Hydraulic	Particle speed cannot exceed the gravity wave speed; gravity plays a crucial role.	Indefinite	$O[(gD)^{1/2}DL]$	Whitehead et al. (1974), Gill (1977), Armi (1986), Farmer and Armi (1986), Armi and Farmer (1986), Pratt (1986)
Geostrophic	Sea-level difference across a channel connecting two basins cannot be greater than the sea-level difference between the basins; gravity plays an important role.	Indefinite	$gD\tilde{\eta}/f$	Garrett and Toulany (1982), Garrett (1983), Garrett and Majaess (1984), Toulany and Garrett (1984), Whitehead (1986).
Vorticity	Intrusion speed cannot exceed limit imposed by the vorticity front; gravity plays *no* role.	Finite (until edge of channel is reached); afterwards one of the other controls will be active.	$\frac{2}{27}\zeta DL^2$	Present article

Here, g is the gravitational acceleration, D the channel depth (i.e., $H + \Delta H$), L the channel width, $\tilde{\eta}$ the sea-level difference between the basins, f the Coriolis parameter and ζ ($=f\Delta H/H$) is the uniform vorticity of the intruding fluid.

(Wolanski 1986). Is it possible that the flow is transient and controlled by the vorticity? With the existing literature it is impossible to answer this question. It is hoped, however, that the theoretical considerations presented here will encourage future investigations of barotropic channel flows so that the question can be answered.

7. Summary

Prior to summarizing our results, it is appropriate to stress once more the main approximations and assumptions involved in our study. The analysis does not include the effects of coastline irregularities, nonuniformities in depth and the unsteadiness of the flow. In reality, these processes will, no doubt, influence the flow. Although much work remains to be done before we can adequately understand the behavior of the real system, our present findings give some useful information.

The results of the theory can be summarized as follows:

(i) When an inviscid fluid with uniform relative vorticity ζ $(=f\Delta H/H)$ intrudes steadily into an otherwise motionless channel, it occupies exactly two-thirds of the channel width (L). When the relative vorticity is cyclonic the intrusion propagates along the right wall and when the vorticity is anticyclonic it propagates along the left wall (Fig. 6).

(ii) The frictionless intrusion propagates at a rate of $\zeta L/9$ and the vorticity front intersects the wall at an angle of exactly 90°.

(iii) The net inviscid mass flux associated with the intrusion is $\frac{2}{27}\zeta DL^2$ (where D is the channel depth). The total flux entering the channel is actually larger, $\frac{8}{81}\zeta DL^2$. Of this larger flux, 25% (i.e., $\frac{2}{81}\zeta DL^2$) is detrained (i.e., it is released by the intruding fluid and absorbed by the fluid in the channel) and 75% into the channel (Fig. 6).

(iv) The above conditions result from a balance between the forward momentum flux associated with the intrusion and the backward form drag exerted (on the intrusion) by the ambient fluid.

(v) When weak dissipation (in the form of laterally breaking waves) is allowed, the intrusion propagation rate is smaller than the inviscid value, the width is narrower than the frictionless width ($2.3L$) and the transport is smaller than the inviscid flux.

(vi) Under no circumstances can the speed, width and flux exceed the values given in (iii). Attempts to force more fluid into the channel (say, by imposing large sea level differences) will be frustrated by an alteration of the upstream conditions.

The above results demonstrate that the intrusion speed and flux are entirely controlled by the relative vorticity of the intruding fluid. A summary of the relationship between our newly proposed vorticity control and the so-called hydraulic control and geostrophic control is given in Table 1. As a point of general interest, it is remarked that purely baroclinic intrusions such as the Skagerrak outflow (Stern 1980, Stern et al. 1982, Kubokawa and Hanawa 1984a,b, Nof 1987) are governed by gravity and are not subject to vorticity control.

For most oceanic channels in midlatitude the vorticity control is much more severe than the hydraulic control. The ratio between the two fluxes is roughly $2L/27R_d$ (where R_d is the barotropic deformation radius). Hence, for a midlatitude channel 20 km broad and 200 m deep, the flux controlled by the vorticity is less than one percent of the hydraulically controlled flux. In view of this, it is suggested that the vorticity can choke the flow in various barotropic channels.

Possible applications of the present theory are mentioned in the section 7. Unfortunately, the lack of temperature signature in barotropic intrusions makes them very difficult to locate and, consequently, there have not been any direction observations. It is hoped that the present study will encourage such observations.

Acknowledgments. This study was supported by the Office of Naval Research (Contract N00014-82-C-0404) and by the Florida State University. The comments of two anonymous reviewers and L. Pratt were very helpful.

REFERENCES

Armi, L., 1986: The hydraulics of two flowing layers with different densities. *J. Fluid Mech.*, **163**, 27–58.

——, and D. M. Farmer, 1986: Maximal two-layer exchange through a contraction with barotropic net flow. *J. Fluid Mech.*, **164**, 27–51.

Borenas, K., and L. Lundberg, 1986: Rotating hydraulics of flow in a parabolic channel. *J. Fluid Mech.*, **167**, 309–326.

Batchelor, G. K., 1967: *An Introduction to Fluid Dynamics.* Cambridge University Press, 615 pp.

Benjamin, T. B., 1968: Gravity currents and related phenomena. *J. Fluid Mech.*, **31**, 209–248.

Farmer, D. M., and L. Armi, 1986: Maximal two-layer exchange over a sill and through the combination of a sill and contraction with barotropic flow. *J. Fluid Mech.*, **164**, 53–76.

Garrett, C. J. R., 1983: Variable sea level and strait flows in the Mediterranean: A theoretical study of the response to meteorological forcing. *Oceanol. Acta*, **6**, 79–87.

——, and F. Majaess, 1984: Non-isostatic response of sea level to atmospheric pressure in the eastern Mediterranean. *J. Phys. Oceanogr.*, **14**, 656–665.

——, and B. Toulany, 1982: Sea level variability due to meteorological forcing in the northeast Gulf of St. Lawrence. *J. Geophys. Res.*, **87**, 1968–1978.

Gill, A. E., 1977: The hydraulics of rotating-channel flow. *J. Fluid Mech.*, **80**, 641–677.

Kubokawa, A., and K. Hanawa, 1984a: A theory of semigeostrophic gravity waves and its application to the intrusion of a density current along a coast. Part I. *J. Oceanogr. Soc. Japan*, **40**, 247–259.

——, and ——, 1984b: A theory of semigeostrophic gravity waves and its application to the intrusion of a density current along a coast. Part II. *J. Oceanogr. Soc. Japan*, **40**, 260–270.

Nof, D., 1987: Penetrating outflows and the dam-breaking problem. *J. Mar. Res.*, in press.

——, and S. Im, 1985: Suction through broad oceanic gaps. *J. Phys. Oceanogr.*, **15**, 1721–1732.

——, and D. Olson, 1983: On the flow through broad gaps with application to the Windward Passage. *J. Phys. Oceanogr.*, **13**, 1940–1956.

Pratt, L., 1983: An inertial flow over topography. Part I: Semigeostrophic adjustment to an obstacle. *J. Fluid Mech.*, **131**, 198–218.

——, 1984: An inertial flow over topography. Part II: Rotating channel flow near the critical speed. *J. Fluid Mech.*, **145**, 95–110.

——, 1986: Hydraulic control of sill flow in the bottom friction. *J. Phys. Oceanogr.*, **16**, 1970–1980.

Sambuco, E., and J. A. Whitehead, 1976: Hydraulic control by a wide weir in a rotating fluid. *J. Fluid Mech.*, **73**, 521–528.

Stern, M. E., 1972: Hydraulically critical rotating flow. *Phys. Fluids*, **15**, 2062–2064.

——, 1974: Comment of rotating hydraulics. *Geophys. Fluid Dyn.*, **6**, 127–130.

——, 1980: Geostrophic fronts, bores, breaking and blocking waves. *J. Fluid Mech.*, **99**, 687–703.

——, 1985: Lateral wave breaking and shingle formation in large scale shear flow. *J. Phys. Oceanogr.*, **15**, 1274.

——, and L. Pratt, 1985: Dynamics of vorticity fronts. *J. Fluid Mech.*, **161**, 513–532.

——, and S. I. Voropayev, 1984: Formation of vorticity fronts in shear flow. *Phys. Fluids*, **27**, 848–855.

——, J. A. Whitehead and B. L. Hua, 1982: The intrusion of a density current along a wall in a rotating fluid. *J. Fluid Mech.*, **123**, 237–265.

Stokes, G. G., 1847: On the theory of oscillatory waves. *Trans. Cambridge Phil. Soc.*, **8**, 441–455.

Thompson, R. E., 1976: Tidal currents and estuarine-type circulation in Johnson Strait, British Columbia. *J. Fish. Res. Board Can.*, **33**, 2242–2264.

Toulany, B., and C. Garrett, 1984: Geostrophic control of fluctuating barotropic flow through straits. *J. Phys. Oceanogr.*, **14**, 649–655.

Von Karman, T., 1940: The engineer grapples with nonlinear problems. *Bull. Amer. Math. Soc.*, **46**, 615.

Whitehead, J. A., 1986: Flow of a homogeneous rotating fluid through straits. *Geophys. Astrophys. Fluid Dyn.*, in press.

——, A. Leetmaa and R. A. Knox, 1974: Rotating hydraulics of strait and sill flows. *Geophys. Fluid Dyn.*, **6**, 101–125.

Wolanski, E. J., 1986: The physical oceanography of Torres Strait. Torres Strait Fisheries Seminar, Port Moresby, 11–14 February 1985, 275–291.